

## APPENDIX

### Stem Design

The Epoch femoral stem (Zimmer, Warsaw, Indiana) is a composite stem made of a core of forged cobalt-chromium alloy surrounded by a layer of polyaryletherketone polymer that is injection-molded onto the metallic core. This core imparts structural durability to the implant while the polyaryletherketone polymer reduces the overall bending stiffness of the implant when compared with that of a solid cobalt-chromium stem<sup>3,4\*</sup>. A full-length, circumferential coating of commercially pure titanium mesh is applied to the polymer by thin film bonding to provide a porous surface for bone ingrowth. This layer has an effective thickness of 0.83 mm and an average pore size of 300  $\mu\text{m}$ . The implant received FDA approval in 2002 for use in the United States.

### Radiographic Evaluation

This assessment included evaluation of calcar remodeling and pedestal formation. The method of Engh et al.<sup>20-22</sup> was used to characterize femoral stem fixation as bone ingrowth, stable fibrous, or unstable fibrous. Radiodense and radiolucent lines around the femoral component were evaluated, and their locations were identified according to the zones described by Gruen et al.<sup>8</sup>. Osteolysis of the pelvis and femur was evaluated according to a modification of the system developed for the American Academy of Orthopaedic Surgeons, as described by Weber et al.<sup>23</sup>. Osteolytic defects were noted if they measured  $\geq 2$  mm in diameter. Vertical migration (subsidence) of the femoral stem was evaluated by measuring the change in the distance between the most proximal point of the lesser trochanter and the most superomedial points of the femoral component on sequential radiographs. On the basis of previously established criteria described by Callaghan et al.<sup>24,25</sup>,  $\geq 5$  mm was considered to indicate subsidence. The classification system of Brooker et al.<sup>9</sup> was used to grade heterotopic ossification when it was present.

Radiolucent lines around the acetabular component were evaluated, and their locations were identified according to the zones described by DeLee and Charnley<sup>10</sup>. Osteolysis of the pelvis was assessed as previously described for osteolysis of the femur. Migration of the acetabular component was evaluated by measuring the vertical distance between the center of the cup and a line joining the teardrops as well as by measuring the horizontal distance between the center of the cup and a vertical line through the teardrop<sup>26</sup>. Migration of  $\geq 5$  mm was considered to be important<sup>26</sup>. The inclination of the acetabular cup from the horizontal (the cup angle) was measured by drawing a horizontal line through both teardrops and another line through the plane opening of the cup. Any change in this angle of  $>5^\circ$  on sequential radiographs was considered important.

### Histologic Analysis

The femora were dehydrated, fixed, and then embedded in polymethylmethacrylate with use of standard histologic methods. Sections, 500  $\mu\text{m}$  thick, were generated at 1-cm intervals proximally to distally along each stem (Fig. E1). Each 500- $\mu\text{m}$ -thick section was mounted and was then sequentially ground and polished. The final thickness of each section was approximately 150  $\mu\text{m}$ . The sections were treated with 0.1% formic acid to decalcify the surface and were then stained with toluidine blue O.

Each section was evaluated for total ingrowth and ongrowth with polarized transmitted light microscopy (Nikon Optiphot-2; Nikon Instruments, Melville, New York) and quantitative image analysis (BQ NOVA PRIME software; Bioquant Image Analysis, Nashville, Tennessee). A 35-mm camera and Kodak T160 Ektachrome slide film (Kodak, Rochester, New York) were used to record microscope field images. The slides were then scanned with a Polaroid Sprint Scanner 35 Plus (Polaroid, Wayland, Massachusetts), and the images were processed in Adobe Photoshop 7.01 (Adobe Systems, San Jose, California).

Montages were constructed for each cross section at two magnifications. The low-magnification ( $0.63\times$  objective) montages encompassed the entire bone and implant cross section and were used to qualitatively evaluate the porosity of the cortical bone. The high-magnification ( $2.5\times$  objective) montages encompassed the titanium mesh and extended to the outer perimeter of the implant and were used to measure bone ingrowth and ongrowth. Fifteen to twenty-five microscope field images were required to fully capture each cross section at these magnifications.

Adobe Photoshop was used to define the region of interest for quantitative analysis of bone ingrowth and bone ongrowth. For bone ingrowth, each component (bone, titanium mesh, polyaryletherketone, and void space) were colorized for unique identification within the region of interest (Fig. E2). The area of the region of interest encompassed all of the titanium mesh as well as the polyaryletherketone, new bone, and void spaces within the mesh. The outer boundary of the region of interest was drawn tangentially to the outer surface of the outermost titanium mesh fibers (Fig. E2). Similarly, the inner boundary was drawn tangentially to the inner surface of the innermost titanium mesh fibers. Following colorization, the area of the region of interest ( $A_{\text{ROI}}$ ) and of the bone, titanium fiber mesh, polyaryletherketone, and void space components ( $A_{\text{bone}}$ ,  $A_{\text{Ti}}$ ,  $A_{\text{PAEK}}$ , and  $A_{\text{voids}}$ , respectively) were determined with use of the Bioquant software ( $A_{\text{ROI}} = A_{\text{bone}} + A_{\text{Ti}} + A_{\text{PAEK}} + A_{\text{voids}}$ ). The extent of error ( $100 \times [A_{\text{ROI}} - (A_{\text{bone}} + A_{\text{Ti}} + A_{\text{PAEK}} + A_{\text{voids}})]/A_{\text{ROI}}$ ) was determined to be less than  $\pm 10\%$ . Bone ingrowth was evaluated as the percent of the initial potential void space ( $A_{\text{initial}} = A_{\text{bone}} + A_{\text{voids}}$ ) within the region of interest that was filled by bone ( $100 \times [A_{\text{bone}}/(A_{\text{bone}} + A_{\text{voids}})]$ ).

For bone ongrowth, the length of the outer perimeter ( $P_{\text{implant}}$ ) and the length of the outer perimeter that was in direct contact with bone outside of the region of interest ( $P_{\text{contact}}$ ) were determined. Bone ongrowth was evaluated as the percentage of bone (outside the region of interest) in contact with the outer perimeter of the region of interest of the implant ( $100 \times P_{\text{contact}}/P_{\text{implant}}$ ).

\*See full text of paper for reference list.

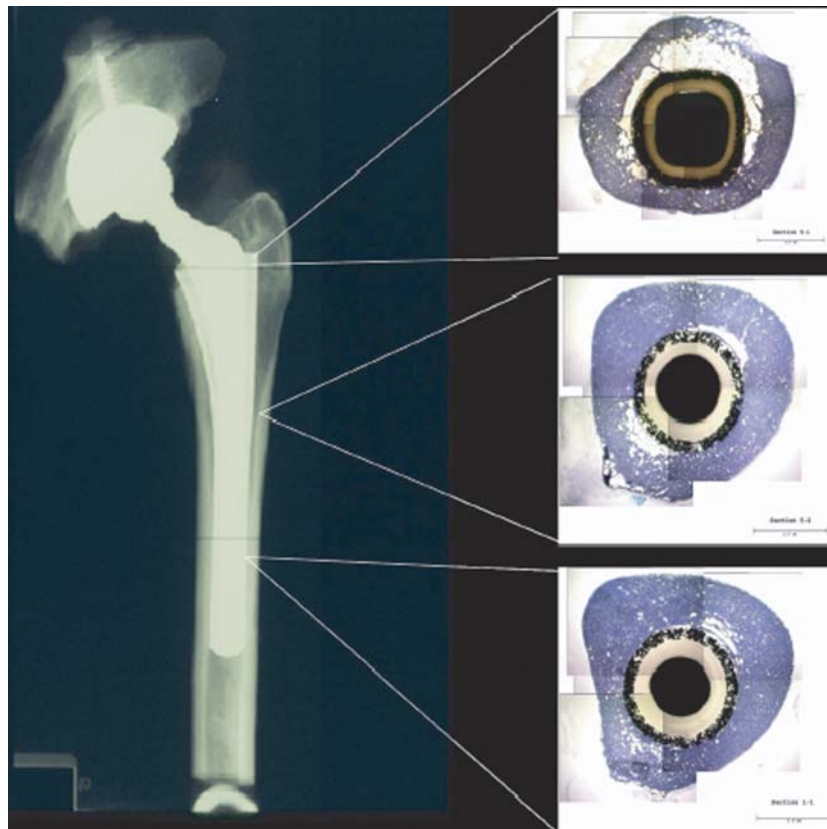


Fig. E-1

Radiograph of the autopsy specimen retrieved at forty-eight months after implantation, with representative sections through the proximal, middle, and distal portions of the Epoch stem.

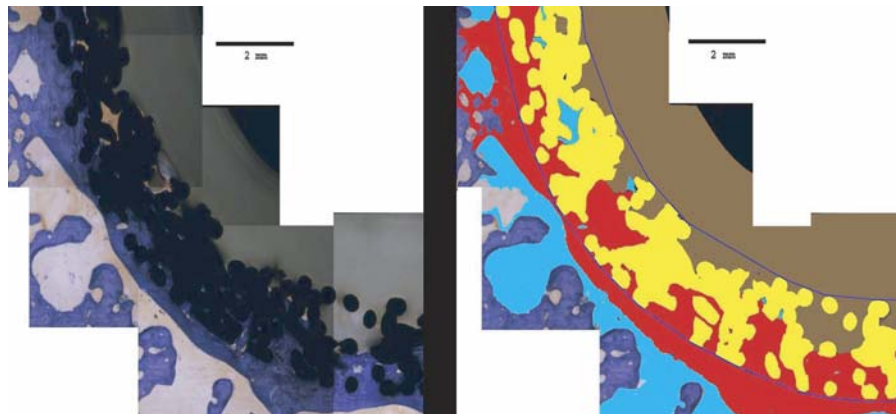


Fig. E-2

*Left:* Light micrograph of the titanium-mesh region of a cross section of the specimen with the Epoch stem retrieved at autopsy forty-eight months after implantation. The image shows bone (purple), metal mesh (black), polyaryletherketone (gray), and void space (tan). *Right:* The same image with the component colorized for quantitative image analysis, showing bone (red), titanium mesh (yellow), polyaryletherketone (tan), and unfilled voids (aqua). Note that the region of interest is defined by the blue borders bracketing the titanium mesh.